A Comparison of Power Density for Axial Flux Machines Based on General Purpose Sizing Equations

Surong Huang* Jian Luo Franco Leonardi** Thomas A. Lipo
Student Member, IEEE *Member, IEEE* *Fellow, IEEE*

*College of Automation
Shanghai University
147 Yan-Chang Road
Shanghai, 200072, P.R.China

**McCleer Power Inc.
2421 Research Drive
Jackson, MI 49203, U.S.A.

Department of Electrical and Computer Engineering
University of Wisconsin-Madison
1415 Engineering Drive
Madison, WI 53706-1691, U.S.A.

Abstract — **Based on the concept of the converter fed machine (CFM), an optimal machine design can be considered as the best match of the machine topology, the power electronic converter and the performance specification. To compare power production potential of axial flux machines with various topologies, different waveforms of back emf and current, general purpose sizing and power density equations for such machines are needed. In this paper, a general approach is presented to develop and to interpret these equations. Sample applications of the sizing and power density equations are utilized to compare the axial flux toroidal permanent magnet (AFTPM) machine and the axial flux two-stator permanent magnet (AF2SPM) machine.**

I. INTRODUCTION

In general, comparison of different machine types is a formidable task since many variables exist for each machine and it is difficult to select those variables which should be held constant for comparison purposes. One traditional method of comparison is to use the $D_g^2 L_e$ sizing equation, which compares the machine power on the basis of air gap surface diameter D_g and effective stack length L_e.

The traditional design of AC electrical machines is based on the premise that the machine has a radial air-gap flux, only one stator and one rotor, and it is supplied by a sinusoidal source. It was recognized in [1] and [2], however that the emergence of power electronic converters has removed the need for such a concept as the basis for machine design. Beginning with the variable reluctance and permanent magnet machines, a new generation of electrical machine has evolved, based on the principle that the best machine design is the one that simply produce the optimum match between the machine and the power electronic converter. In particular, promising developments in the field of axial flux PM machines has raised issues concerning the power density of such machines when compared with more conventional topologies [5,6].

With the evolution of converter fed machines (CFMs), it becomes important to compare power potential of machines with vastly different topologies, having a variety of different waveforms of back emf and current. In 1996, S. Huang et al. [3] developed the general purpose sizing and power density equations and introduced a systematic method to compare the capabilities of machines with different topologies. The power density was compared on the basis of total occupied volume instead of air gap volume. Special factors were introduced to account for the effects of non-sinusoidal current and back emf waveforms. As a further study, a detailed approach will be presented in this paper for the application of the general purpose sizing and power density equations to axial flux machines, focusing specifically on the axial flux toroidal permanent magnet (pm) machine (AFTPM) and the axial flux dual stator pm machine (AF2SPM).

PE-621-EC-0-08-1997 A paper recommended and approved by the IEEE Electric Machinery Committee of the IEEE Power Engineering Society for publication in the IEEE Transactions on Energy Conversion. Manuscript submitted September 3, 1996; made available for printing September 10, 1997.

II. SIZING EQUATIONS AND POWER DENSITIES

The general purpose sizing equations for radial gap machines take the form, [3]

$$P_R = \frac{1}{1+K_\phi}\frac{m}{m_1}\frac{\pi}{2}K_e K_i K_p \eta B_g A \frac{f}{p}\lambda_o^2 D_o^2 L_e \qquad (1)$$

and

$$P_R = \frac{1}{1+K_\phi}\frac{m}{m_1}\frac{\pi}{2}K_e K_i K_p k_l \eta B_g A \frac{f}{p}\lambda_o^3 D_o^3 \qquad (2)$$

where

- K_ϕ ratio of electrical loading on rotor and stator. (In a machine without a rotor winding, K_ϕ=0.)
- m number of phases of the machine.
- m_1 number of phases of each stator (if there is more than one stator, each stator has the same m_1).
- K_e emf factor incorporating the winding distribution factor K_w and the ratio between the area spanned by the salient poles and the total airgap area
- K_i current waveform factor.
- K_p electrical power waveform factor.

η machine efficiency.
B_g flux density in the air gap.
A total electrical loading including both the stator electrical loading A_s and rotor electrical loading A_r.
f converter frequency.
p machine pole pairs.
D_o diameter of the outer surface of the machine.
L_e effective stack length of the machine.
k_l aspect ratio coefficient L_e/D_g of the effective stack length over the gap diameter in radial air-gap machines.
λ_o ratio of the diameter of the air-gap surface vs. the diameter of the outer surface of the machine.

If stator leakage inductance and resistance are neglected, the output power for any electrical machine can be expressed as [3]

$$P_R = \eta \frac{m}{T} \int_0^T e(t)\, i(t)\, dt = \eta\, m\, K_p\, E_{pk}\, I_{pk} \qquad (3)$$

where emf $e(t)$ and E_{pk} are the phase air-gap emf and its peak value. The currents $i(t)$ and I_{pk} are the phase current and the peak phase current, and T is the period of one cycle of the emf. The factor K_p is defined as

$$K_p = \frac{1}{T} \int_0^T \frac{e(t) \times i(t)}{E_{pk} \times I_{pk}}\, dt = \frac{1}{T} \int_0^T f_e(t)\, f_i(t) dt \qquad (4)$$

where $f_e(t)=e(t)/E_{pk}$ and $f_i(t)=i(t)/I_{pk}$ are the expressions for normalized emf and current waveforms.

The emf in Eq. (3) for the axial flux machines is given by

$$e(t) = \frac{d\Lambda_g}{dt} = K_e N_t B_g \frac{f}{p} (1-\lambda^2) D_o^2 f_e(t) \qquad (5)$$

where Λ_g is the air-gap flux linkage per phase, N_t is the number of turns per phase. The ratio λ is defined as

$$\lambda = \frac{D_i}{D_o} \qquad (6)$$

where D_i is the inner diameter of the machine. From Eq. (5) it is apparent that

$$E_{pk} = K_e N_t B_g \frac{f}{p} (1-\lambda^2) D_o^2 \qquad (7)$$

The factor K_i is defined as [3]

$$K_i = \frac{I_{pk}}{I_{rms}} = \left(\frac{1}{T} \int_0^T \left(\frac{i(t)}{I_{pk}}\right)^2 dt\right)^{-1/2} \qquad (8)$$

where I_{rms} is the rms phase current which is related to the stator electrical loading A_s. For the axial flux machines the electrical loading A_s is a function of radius. Its average is

$$A_s = 2 m_1 N_t \frac{I_{rms}}{\pi D_g} \qquad (9)$$

where the average diameter of air gap is

$$D_g = \frac{D_o + D_i}{2} = \frac{1+\lambda}{2} D_o \qquad (10)$$

In the general case, the total electrical loading A should include both the stator electrical loading A_s and rotor electrical loading A_r so that [3],

$$A_s = A - A_r = \frac{A}{1+K_\phi} \qquad (11)$$

By Eqs. (8),(9) and (11) an expression for the peak current is

$$I_{pk} = \frac{1}{1+K_\phi} K_i A\, \pi \frac{D_g}{2 m_1 N_t} \qquad (12)$$

Combining Eqs. (3), (7), (10), (12), the general purpose D_o^3 sizing equation for the axial flux machines takes the form of

$$P_R = \frac{1}{1+K_\phi} \frac{m}{m_1} \frac{\pi}{2} K_e K_i K_p \eta B_g A \frac{f}{p} (1-\lambda^2) \frac{1+\lambda}{2} D_o^3 \qquad (13)$$

To realize the required $D_o^2 L_e$ sizing equation, it is useful to define the ratio K_L considering the duality of the axial flux and the radial flux machines

$$K_L = \frac{D_o}{L_e} = f(L_s, L_r, L_{PM}, \lambda, D_o, g, p) \qquad (14)$$

where

L_s axial length of the stator.
L_r axial length of the rotor.
L_{PM} axial length of the permanent magnet (if any).
g axial length of the air gap.

A procedure needs to be developed to determine K_L when studying a specific machine or structure. This procedure will incorporate the effects of temperature rise, losses, and efficiency requirements on the design. In practice, the lengths L_s and L_r depend upon the stator equivalent electrical loading A_s, the current density J_s, the slot fill factor K_{cu}, and flux densities in the different parts of the machine. The length L_{PM} depends on the air gap flux density and air gap length. The outer diameter D_o is determined by Eq. (13).

In most axial flux machines, the ratio λ is a major design parameter which has significant effect on the characteristics of the machine. To optimize machine performance, the value of λ must be carefully chosen. For many years, researchers have been interested in choosing an optimal value of the ratio λ to yield the best electrical and magnetic loading for an axial flux machine. In 1974 P. Campbell derived an optimized value of $\lambda = 1/\sqrt{3}$ for the maximum armature power in a permanent magnet axial field DC machine [4]. However, the length of the machine was not accounted for in this analysis and thus the concept of power density was not applied. In 1994 F. Caricchi et al. presented an optimized

value of the ratio λ=0.63 for AFTPM machine, to achieve a high value of both the torque and torque-to-weight ratio [5].

In practice, the optimal value of λ is different depending upon the optimization goal. Moreover, for given electrical loading and flux densities, even when the optimization criterion is the same the optimal value of λ also differs for different rated power, pole pairs, converter frequency etc. Further, if different materials or different structures are involved, the optimal λ will have a significantly different value.

The final general purpose sizing equation ultimately takes the form of

$$P_R = \frac{1}{1+K_\phi}\frac{m}{m_1}\frac{\pi}{2}K_e K_i K_p K_L \eta B_g A \frac{f}{p}(1-\lambda^2)\frac{1+\lambda}{2}D_o^2 L_e \qquad (15)$$

The overall power density of axial flux machine can be defined as

$$\xi = \frac{P_R}{\frac{\pi}{4}D_t^2 L_e} \qquad (16)$$

where D_t is the total outer diameter of the machine including the stack outer diameter and the protrusion of the end winding from the iron stack in the radial direction.

By examining the back emf and current waveform for a particular machine type, the factors, K_i and K_p in the sizing equation can be determined. Typical waveforms and their corresponding K_i and K_p from Ref. [3] are shown in Table I.

TABLE I
TYPICAL PROTOTYPE WAVEFORMS

Model	e(t)	i(t)	K_i	K_p
Sinusoidal waveform	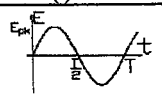	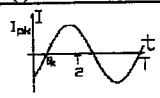	$\sqrt{2}$	$\frac{1}{2}\cos\phi$
Sinusoidal waveform	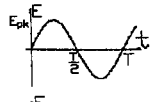	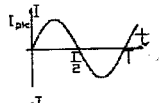	$\sqrt{2}$	0.5
Rectangular waveform	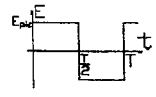	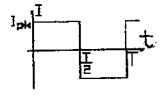	1	1
Trapezoidal waveform	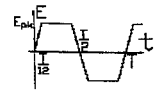	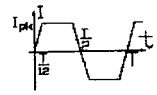	1.134	0.777
Triangular waveform	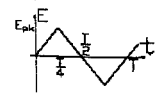	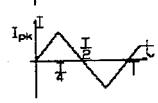	$\sqrt{\ }$	0.333

III. APPLICATION OF THE GENERAL PURPOSE SIZING EQUATION TO AFTPM MACHINES

The concept of the axial flux toroidal permanent magnet (AFTPM) machine was presented in Refs. [1], [5] and [6].

The AFTPM topology is shown on Fig. 1. The machine total outer diameter D_t is given by

$$D_t = D_o + 2W_{cuo} \qquad (17)$$

where W_{cuo} is the protrusion of the end winding from the iron stack in the radial direction. Protrusions exist toward the axis of the machine as well as toward the outside: their amplitude depend on the stator equivalent electrical loading A_s, the current density J_s, and the copper fill factor K_{cu}, as shown in Eq. (18)

$$\left.\begin{aligned} W_{cui} &= \frac{\sqrt{D_i^2 + \frac{4A_s D_g}{K_{cu}J_s}} - D_i}{2} \\ W_{cuo} &= \frac{\sqrt{D_o^2 + \frac{4A_s D_g}{K_{cu}J_s}} - D_o}{2} \end{aligned}\right\} \qquad (18)$$

The axial length of the machine is given by

$$L_e = L_s + 2L_r + 2g \qquad (19)$$

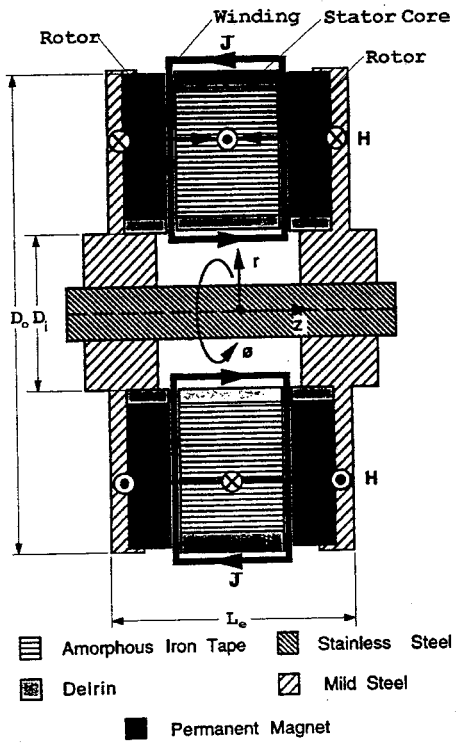

Fig. 1 AFTPM Machines

From manufacturing experience, the axial length of the stator can be approximated by

$$L_s = L_{cs} + 1.6W_{cui} \quad (20)$$

where L_{cs} is the axial length of the stator core.

$$L_{cs} = \frac{B_g \pi D_o (1+\lambda)}{B_{cs} 4p} \quad (21)$$

where B_{cs} is the flux density in the stator core.

The axial length of rotor L_r is given by

$$L_r = L_{cr} + L_{PM} \quad (22)$$

where L_{cr} is the axial length of rotor disc core. The PM length L_{PM} can be calculated as [7]

$$L_{PM} = \frac{\mu_r B_g}{0.95B_r - \frac{1}{K_d} B_u}(g + W_{cui}) \quad (23)$$

where μ_r is the recoil relative permeability of the permanent magnet, B_r is the residual flux density and depends on PM material, B_u is the attainable flux density on the surface of the permanent magnets, and K_d is the flux leakage factor of the PM machines obtained through a finite element study or through design experience. [In a very simplified approach K_d can be taken as (1-p/30)]

The axial length of rotor disc core L_{cr} is expressed as

$$L_{cr} = \frac{B_u \pi D_o (1+\lambda)}{B_{cr} 8p} \quad (24)$$

where B_{cr} is the flux density in the rotor disc core.

Combining Eqs. (18) to (24) the axial length L_e is

$$L_e = \frac{\pi D_o (1+\lambda)}{4p}\left(\frac{B_g}{B_{cs}} + \frac{B_u}{B_{cr}}\right) + (1.6W_{cui} + 2g) \times \left(1 + \frac{\mu_r B_g}{0.95B_r - \frac{1}{K_d} B_u}\right) \quad (25)$$

Referring to Eq. (14) the aspect ratio K_L can be derived as

$$K_L = \left(\frac{\pi(1+\lambda)}{4p}\left(\frac{B_g}{B_{cs}} + \frac{B_u}{B_{cr}}\right) + \frac{1}{D_o}(1.6W_{cui} + 2g) \times \left(1 + \frac{\mu_r B_g}{0.95B_r - \frac{1}{K_d} B_u}\right)\right)^{-1} \quad (26)$$

Due to the structure of an AFTPM machine, the flux in the stator and rotor have different characteristics. In the stator core an AC flux exists while on the other hand in the rotor disc core a nearly constant flux exists. The relationship between flux density B_{cs} and converter frequency f can be estimated by [3]

$$B_{cs} = \begin{cases} 5.47 f^{-0.32} & f > 40Hz \\ 1.7 \text{ to } 1.8 & f \le 40Hz \end{cases} \quad (27)$$

The flux density in the rotor disc core should be set to

$$B_{cr} = 1.6 \text{ to } 1.8 \quad (28)$$

The air gap flux density B_g can also be expressed as

$$B_g = K_{focus} B_u \quad (29)$$

where K_{focus} is the flux focusing factor which is related to the structure of the permanent magnet machine. Generally [3]

$$K_{focus} = \frac{A_{pm}}{A_p} K_d \quad (30)$$

where A_{pm} is the surface area of permanent magnets, A_p is the area of the gap surface physically crossed by the flux. For a surface mounted machine like the AFTPM it is $A_{pm} = A_p$ (Fig. 1). Because the AFTPM machine does not have the capability of flux focusing, rare earth permanent magnets can be used to increase the power density. For the AFTPM (Fig. 1), it can be determined that $K_e = \pi$. As there is no rotor winding $K_\phi = 0$. Considering the trapezoidal waveforms in Table I (row 4), $K_i K_p = 0.881$. From Eqs. (15), (29) and (30), the following AFTPM machine sizing equation is obtained

$$P_{R(AFTPM)} = 0.22\,\pi^2\,\eta\,K_d\,B_u\,A\frac{f}{p}\,K_L(1-\lambda^2)(1+\lambda)\,D_o^2 L_e \quad (31)$$

and the power density of the AFTPM machine is

$$\xi_{(AFTPM)} = 0.881\,\pi\,\eta\,K_d\,B_u\,A\frac{f}{p}\,K_L(1-\lambda^2)(1+\lambda)\,\frac{D_o^2}{D_i^2} \quad (32)$$

In Eqs. (31) and (32), the only independent term is λ while the other terms either depend on λ or have certain physical limitations. The relationships between power density and efficiency of the AFTPM machine vs. ratio λ are shown on Fig. 2, respectively. It is very clear that the ratio λ has a more significant effect on power density than on efficiency. It should be noted that, because of the curve of efficiency vs. λ has a flat shape, from the design point of view it is advantageous to choose an optimal value of λ to achieve the maximum power density. Further research also shows the close connection between the optimal value of λ and the pole pairs of the machines. Equation (33) gives the recommended optimal value of λ for AFTPM machines with different pole pairs, for the case specified in Fig. 2.

$$\lambda = \frac{D_i}{D_o} = \begin{cases} 0.315 & p = 2 \\ 0.35 & p = 3 \\ 0.375 & p = 4 \\ 0.405 & p = 6 \end{cases} \quad (33)$$

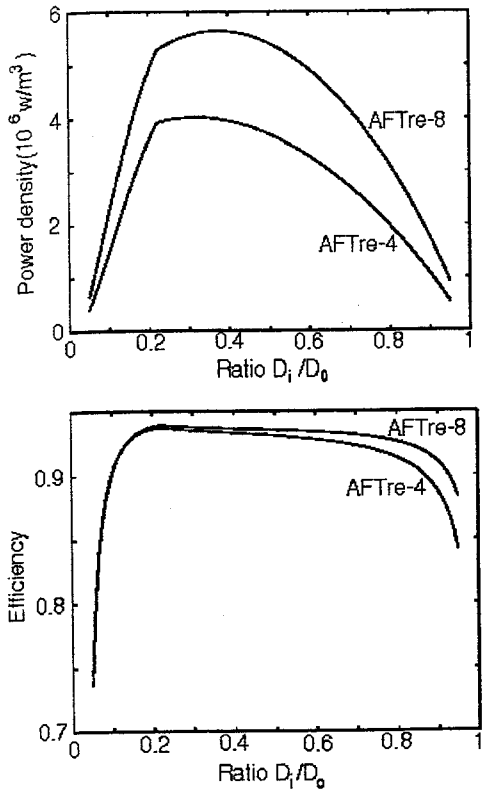

Fig. 2 Power density and efficiency of the AFTPM machine vs. ratio λ. $A = 60{,}000 A/m$, $J_s = 6.2 \times 10^6 A/m^2$, $P_R = 75{,}000\ w$, n_s=3000 rpm, p= 2(AFTre-4), p= 4(AFTre-8), using rare earth PM.

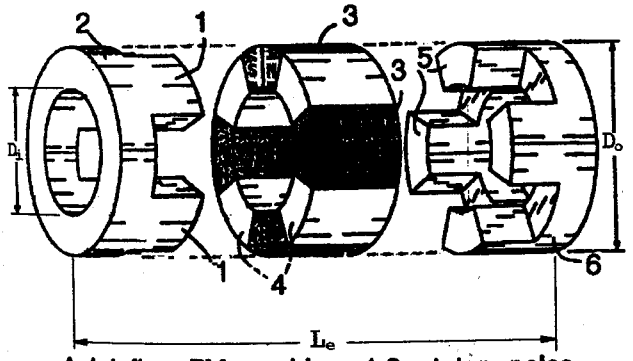

Axial flux PM machine. 1,2 stator poles, 3, ferrite magnets, 4, rotor pole pieces, 5,6 stator poles.

Fig. 3 AF2SPM Machines

IV. APPLICATION OF THE GENERAL SIZING EQUATION TO AF2SPM MACHINES

The concept of an axial flux two-stator permanent magnet (AF2SPM) machine has been discussed in Ref. [8]. The AF2SPM topology is shown on Fig. 3. The machine total outer diameter D_t is given by

$$D_t = D_o + 2W_{cu} \tag{34}$$

Inspecting the AF2SPM stator configuration (Fig. 3), it can be assumed that the protrusion of the end winding from the iron stack in the radial direction is half the value of the stator pole inner arc, that is

$$W_{cu} = \frac{\pi D_o \lambda}{8p} \tag{35}$$

The axial length of the machine is given by

$$L_e = L_r + 2L_s + 2g \tag{36}$$

The axial length of rotor depends on flux focusing factor K_{focus} and pole pairs by

$$L_r = \frac{\pi}{16p} D_o (1+\lambda) \frac{K_{focus}}{K_d} \tag{37}$$

The most interesting feature of this machine is that the factor K_{focus} can easily be adjusted by changing the axial length of the rotor to obtain the desired flux density in the air gap. It illustrates a new concept of flux-focusing structure and is very suitable for ferrite magnets.

The axial length of stator L_s is given by

$$L_s = d_{cs} + d_{ss} \tag{38}$$

where the depth of stator core d_{cs} is

$$d_{cs} = \frac{\pi}{16p} D_o (1+\lambda) K_{focus} \frac{B_u}{B_{cs}} \tag{39}$$

and the depth of stator slot d_{ss} is

$$d_{ss} = \frac{A}{2J_s K_{cu}} \frac{1+\lambda}{\lambda} \tag{40}$$

Combining Eqs.(36) to (40), the axial length L_e is

$$L_e = \frac{\pi}{16p} D_o (1+\lambda) K_{focus} \left(\frac{1}{K_d} + 2\frac{B_u}{B_{cs}}\right) + \frac{A}{J_s K_{cu}} \frac{1+\lambda}{\lambda} + 2g \tag{41}$$

From Eq. (14) the aspect ratio of the AF2SPM machine is

$$K_L = \left(\frac{\pi}{16p}(1+\lambda) K_{focus} \left(\frac{1}{K_d} + 2\frac{B_u}{B_{cs}}\right) + \frac{1}{D_o}\left(\frac{A}{J_s K_{cu}} \frac{1+\lambda}{\lambda} + 2g\right)\right)^{-1} \tag{42}$$

The aspect ratio K_L depends on electrical loading A_s, current density J_s, and the distribution of flux density on the different part of the machine in a manner similar to the AFTPM machines. Also, because the axial length of the rotor is related to the flux-focusing factor K_{focus}, the ratio K_L is largely affected by the material selected.

Due to the doubly salient structure, the flux densities in the stator teeth (B_{ts}), in the air gap (B_g), and in the rotor teeth (B_{tr}) have the same value. The choice of the flux density in the stator tooth can be estimated by [3]

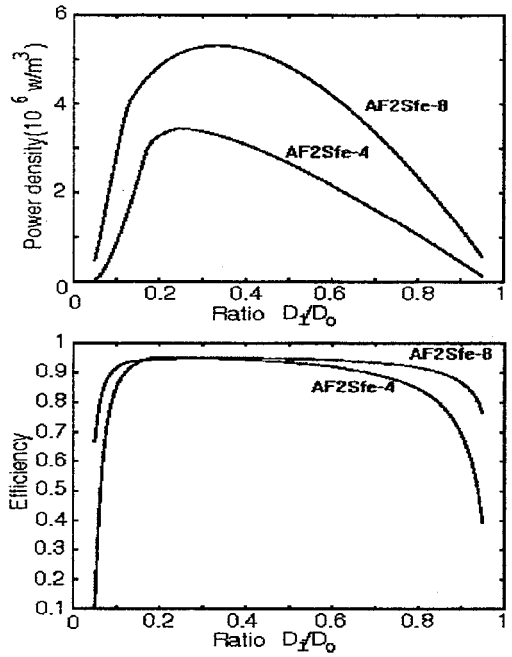

Fig. 4 Power density and efficiency of the AF2SPM machine vs. ratio λ. $A = 60{,}000 A/m$, $J_s = 6.2 \times 10^6\ A/m^2$, $P_R = 75{,}000\ w$, n_s=3000 rpm, p= 2(AF2Sfe-4), p= 4(AF2Sfe-8), using ferrite PM.

$$B_{ts} = \begin{cases} 5.47 f^{-0.32} & f > 40Hz \\ 1.7 \text{ to } 1.8 & f \le 40Hz \end{cases} \qquad (43)$$

and the flux density in stator core

$$B_{cs} = \begin{cases} 4.38 f^{-0.32} & f > 40Hz \\ 1.7 \text{ to } 1.8 & f \le 40Hz \end{cases} \qquad (44)$$

For the AF2SPM topology (Fig. 3), it can be determined that $K_e = \pi/4$, the number of phases of the machine is m=2, the number of phases of each stator is m_1=1. Because there is no rotor winding K_ϕ= 0. Considering the trapezoidal waveforms in Table I (row 4), it can be determined that $K_i K_p$ = 0.881. From Eq. (15), the following AF2SPM machine sizing equation is then obtained

$$P_{R(AF2SPM)} = 0.11\,\pi^2\,\eta\,B_g A \frac{f}{p} K_L(1-\lambda^2)(1+\lambda)\,D_o^2 L_e \qquad (45)$$

and the power density of the AF2SPM machine is

$$\xi_{(AF2SPM)} = 0.441\,\pi\,\eta\,B_g A \frac{f}{p} K_L(1-\lambda^2)(1+\lambda)\frac{D_o^2}{D_i^2} \qquad (46)$$

In Eqs. (45) and (46), similar to AFTPM machine, the only independent term is λ. The power density and efficiency curves of the AF2SPM machine vs. ratio λ using ferrite permanent magnets are shown on Fig. 4, respectively.

The recommended optimal values of the ratio λ for AF2SPM machines with different pole pairs are given in Eq. (47). It is apparent that the optimal values also depend on rated mechanical speed for AF2SPM machines.

$$\lambda = \frac{D_i}{D_o} = \begin{cases} 0.1039 n_s^{0..1014} & p = 2 \\ 0.1188 n_s^{0.1277} & p = 4 \end{cases} \quad Ferrite \quad Magnets$$
$$\begin{cases} 0.0960 n_s^{0.1309} & p = 2 \\ 0.1702 n_s^{0.0983} & p = 4 \end{cases} \quad Rare-earth \quad Magnets \qquad (47)$$

V. COMPARISON BETWEEN INDUCTION AND AXIAL FLUX MACHINES

It is now possible to compare the power densities of AFTPM machines and AF2SPM machines through the use of the sizing and power density equations. Because the squirrel cage induction machine is regarded as the "workhorse" of the ac machine community, it can be considered as a point of reference for the other machines. Figure 5 shows the comparison of power densities among the 4 pole induction machines (IM-4) (Ref.[3]), the 4 pole AFTPM machines with rare earth magnet (AFTre-4) and the 8 pole AFTPM machines with rare earth magnet (AFTre-8). Every point in the curve represent a different machine design optimized for that particular rated mechanical speed. A power density improvement of nearly a factor of three can be achieved for the machine rated at 6000 rpm.

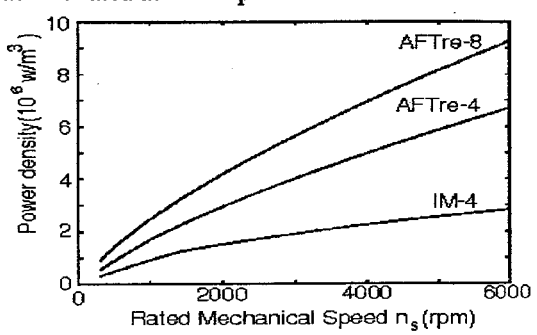

Fig. 5 Power densities comparison between induction machines and AFTPM machines ($A = 60{,}000 A/m$, $J_s = 6.2 \times 10^6\ A/m^2$, P_R = 75,000 w).

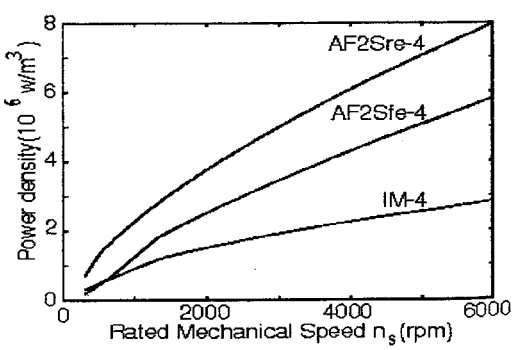

Fig. 6 Power densities comparison between induction machines and AF2SPM machines. ($A = 60{,}000 A/m$, $J_s = 6.2 \times 10^6\ A/m^2$, P_R = 75,000 w.)

Figure 6 shows the comparison of power densities among the 4 pole induction machines (IM-4), the 4 pole AF2SPM

machines with rare earth magnet (AF2Sre-4) and with ferrite magnet (AF2Sfe-4). Taking the 3600rpm machine as an example, our best design for the IM has a stack length of 9.5" and a diameter of 17.5", while the AF2Sre-4 has an axial length of 13" and a diameter of 11".

Clearly, the choice of the most suitable material remains application dependent. Although the machines with rare earth magnet can achieve higher power density, it is apparent that the utilization of a ferrite magnet being much more economical has clear advantages over conventional machines. However it important to mention that due to a considerable axial force that causes vibration and bearing trust, the AF2SPM machines is suitable only for small power ratings.

VI. CONCLUSION

In this paper, the following results have been obtained:

1. A detailed approach is outlined to size axial flux machines by means of general purpose sizing and power density equations [3]. The sizing equations for axial flux machines take a form similar to the general purpose sizing equations for radial flux machines. Such equations permit a comparison of the power capability of different machine topologies based upon overall occupied volume.
2. It is shown that the ratio $\lambda=D_i/D_o$ has a strong effect on the power density and has relatively less effect on machine efficiency. Optimization of λ will achieve a maximum power density as well as nearly the highest efficiency. This result implies that compared to the traditional optimization method, an optimization based on the new sizing equations has distinct advantages, particularly for axial flux machines.
3. It is argued that the optimal value of λ depends upon electrical loading, flux density, frequency, materials, and machine topology etc. and cannot be reduced to a simple numeric value as previously reported. However it is highly dependent on the machine topology and remains in a relatively narrow band.
4. It is shown in the paper that both the axial machines have higher power density than the traditional induction machine particularly when a rare earth magnet is applied and the degree of improvement could reach a factor of three. If cost is a dominating factor, the power density still increases by a factor of two with a ferrite magnet.

REFERENCES

[1] T. A. Lipo and Yue Li, "CFMs - A New Family of Electrical Machines", IPEC'95, Japan, April 3-7, 1995, pp. 1-8.

[2] T. A. Lipo and F. X. Wang, "Design and Performance of Converter Optimized AC Machines", IEEE Trans. on Industry Applications, vol. IA-20, No. 4 July/August 1984, pp. 834-844.

[3] S. Huang, J. Luo, F. Leonardi, and T. A. Lipo, "A General Approach to Sizing and Power Density Equations for Comparison of Electrical Machines", IEEE-IAS Annual Meeting, San Diego, CA Oct. 1996. pp. 836-842.

[4] P. Campbell, "Principle of a Permanent Magnet Axial Field DC Machine", Proc. Inst. Elec. Eng., vol. 121, No. 12, Dec. 1974, pp. 1489-1494.

[5] C. C. Jensen, F. Profumo and T. A. Lipo, " A Low Loss Permanent Magnet Brushless DC Motor Utilizing Tape Wound Amorphous Iron", IEEE Trans. on Industry Applications, vol. 28, No 3, May/June. 1992, pp. 646-651.

[6] F. Caricchi, F. Crescimbini, E. Fedeli and G. Noia, "Design and Construction of a Wheel-Directly-Coupled-Axial-Flux PM Motor Prototype for Evs", IEEE-IAS Annual Meeting, Denver CO, Oct. 1994, pp. 254-261.

[7] Y. Dote, S. Kinoshita, " Brushless Servomotors Fundamental and Applications", Clarendon Press, Oxford, 1990.

[8] Yue Li, "Design and Control of A New Class of Doubly Salient Permanent Magnet Machine", Ph. D. Thesis, University of Wisconsin-Madison, 1995.

[9] E. Spooner, B. J. Chalmers, "Toroidally-Wound, Slotless,Axial-Flux, Permanent-Magnet, Brushless-DC Motors", Proc. Of the International Conference on Electrical Machines, 1988, Vol. III, pp. 81-86.

[10] C. C. Chan, "Axial-Field Electrical Machines - Design and Applications", IEEE Trans. On Energy Conversion, Vol. EC-2, No. 2, June 1987, pp. 294-300.

Surong Huang was born in Shanghai, China, He received the B.S., M.S. degrees in the electrical engineering from the Shanghai University, Shanghai, China. From 1995 to 1996, he worked as a visiting faculty at the University of Wisconsin-Madison. At present, he is an Associate Professor, College of Automation, Shanghai University, Shanghai, China. His research interests are motor and drive design, power electronics and power systems.

Jian Luo was born in Chengdu, China. He received his B.S. degree from the Tsinghua University, Beijing, China, in 1984, and then M.S. degree from the First Academy of Aerospace Industry, Beijing, China, in 1987, both of electrical engineering. From 1987 to 1992, he worked as an electrical engineer in Beijing Institute of Control Device, Beijing, China. Now he is a Ph.D. Student at the University of Wisconsin-Madison. His area of interests includes Optimized electrical machine and drive design, modeling and simulation.

Franco Leonardi received is degree and is doctorate in Electrical Engineering from the Universita' degli Studi di Padova, in 1991 and 1995 respectively. From 1994 to the early 1996 he was at the University of Wisconsin, where under the direction of Prof. T.A. Lipo he worked on Synchronous Reluctance and Doubly Salient Permanent Magnet Motors. In 1996 he joined McCleer Power Inc. where he is currently working on the development of the DSPM technology for traction applications, and other research projects.

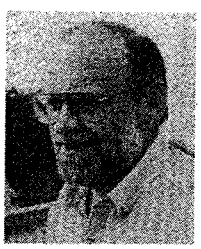

Thomas A. Lipo (M'64-SM'71-F'87) is a native of Milwaukee, WI.

From 1969 to 1979, he was an Electrical Engineer in the Power Electronics Laboratory, Corporate Research and Development, General Electric Company. Schenectady NY. He became Professor of Electrical Engineering at Purdue University, West Lafayette, IN. in 1979, and in 1981 he joined the University of Wisconsin, Madison, in the same capacity, where he is presently the W. W. Grainger Professor for Power Electronics and Electrical Machines.

Dr. Lipo has received the Outstanding Achievement Award from the IEEE Industry Applications Society, the William E. Newell Award of the IEEE Power Electronics Society, and the 1995 Nicola Tesla IEEE Field Award from the IEEE Power Engineering Society for his work. Over the past 30 years he has served IEEE in numerous capacities including President of the Industry Application Society.

Discussion

J. F. Szablya (University of Washington, Bellevue, WA): The authors should be congratulated for this most interesting paper. I have only one comment and associated question.

The number/quantity which indicates the level of utilization of an electric machine is its torque divided by its volume shown in Figures 1 and 2. These figures were derived from the author's Figures 5 and 6, respectively, by dividing their Power Density with the mechanical angular velocity i.e. RPM/(60/2π). This utilization factor is used by machine designers to compare machines of different designs.

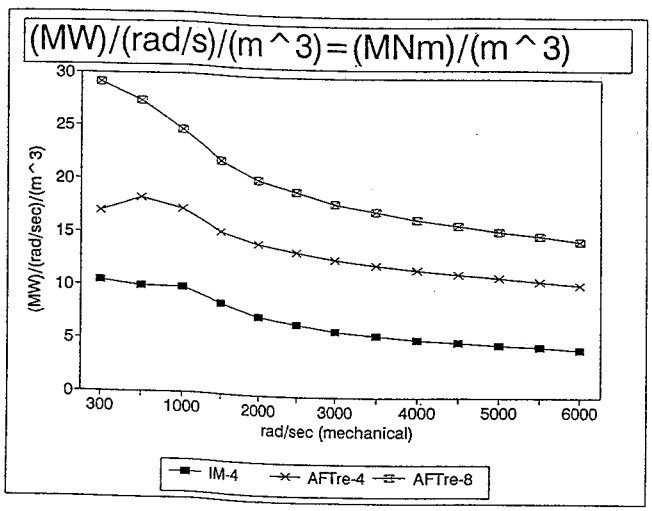

Figure 1

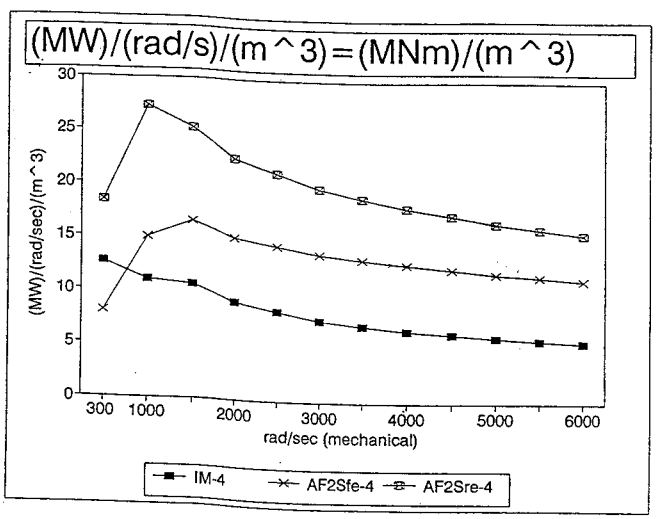

Figure 2

In case of an "ideal machine" or assuming secondary effects (cooling, friction, etc.) to remain same, this utilization factor is not a function of the angular velocity of the shaft, provided the magnetic flux density and the current distributions are kept constant. Even in case of a "real machine" the utilization factor is quite constant over a wide range of RPMs, if any, it will slightly increase with increasing RPM, and will decline at low and high RPMs only due to secondary effects like reduced cooling at lower RPMs, and high windage and friction at high RPMs.

However, the curves in Figures 1 and 2 are not straight, horizontal lines nor do they increase with increasing RPM. To the contrary, they increase considerably towards the lower RPMs and start to decline at very low RPMs only. I would be interested to know what the physical explanation of this interesting behavior of the curves is?

S. Huang, F. Leonardi, D. Qin, and **T. A. Lipo**: The authors wish to thank Prof. Szablya for a timely question, that allows them to clarify an important aspect of the present paper. The comment on the torque density of a machine being constant over a wide speed range is certainly true and a valid point. However as stated in the paper, section V, "Every point in the curve (of figs. 5 and 6) represent a different machine design, optimized for that particular rated mechanical speed." Hence, the curves of figs. 5 and 6 do not represent the power density of a single machine over its speed range, but a curve that is meant to be indicative of a given machine topology, where the best possible power density is searched, while keeping the efficiency and the temperature rise at comparable levels. The size and shape of the optimized design therefore changes with the speed. The magnetic and electrical loading are also adjusted as well to avoid excessive iron losses at high speed. The latter is also the main reason for the lower torque density of the high speed design where iron saturation must be reduced.

Manuscript received April 10, 1998.